PROCEEDINGS OF SCIENCE

H1 measurements of D^* cross sections and $F_2^{c\bar{c}}$ at high Q^2

Martin Brinkmann[*†]
Deutsches Elektronen-Synchroton (DESY)
E-mail: martin.brinkmann@desy.de

The inclusive production of $D^{*\pm}(2010)$ mesons in deep inelastic $e^{\pm}p$ scattering at HERA is measured in the kinematic region of photon virtuality $100\,\mathrm{GeV}^2 < Q^2 < 1000\,\mathrm{GeV}^2$ and inelasticity $0.02 < y < 0.7$. Single and double differential cross sections for inclusive D^* meson production are measured in the visible range defined by $|\eta(D^*)| < 1.5$ and $p_t(D^*) > 1.5\,\mathrm{GeV}$. The data were collected by the H1 experiment during the period from 2004 to 2007 and correspond to an integrated luminosity of $351\,\mathrm{pb}^{-1}$. The charm contribution, $F_2^{c\bar{c}}$, to the proton structure function F_2 is determined. The measurements are compared with QCD predictions.

XVIII International Workshop on Deep-Inelastic Scattering and Related Subjects
April 19 -23, 2010
Convitto della Calza, Firenze, Italy

[*]Speaker.
[†]for the H1 Collaboration

1. Introduction and Theoretical Models

Heavy flavour production in ep collisions at HERA is dominated by boson gluon fusion (BGF), i.e. $\gamma g \to Q\overline{Q}$, in leading order (LO) pertubative quantum chromodynamics (pQCD) in the massive scheme. This process constrains the gluon density in the proton as demonstrated in previous analyses at lower photon virtuality Q^2 [1]. A proper treatment of charm and beauty quarks in pQCD models is one of the central issues in the determination of the parton distribution functions (PDFs) of the proton. The measurement of charm production at large photon virtualities allows to test the reliability of the pQCD calculations in the massive and massless schemes for $Q^2 \gg 4m_c^2$.

The current analysis [2] uses data collected with the H1 detector at HERA during the running periods of 2004-2007 when HERA operated with 27.5 GeV electrons and 920 GeV protons colliding at a centre of mass energy of $\sqrt{s} = 319\,\text{GeV}$. The integrated luminosity for this analysis is $\mathscr{L} = 351\,\text{pb}^{-1}$. Charm events are tagged via fully reconstructed $D^{*\pm}$ mesons using the "golden" decay channel $D^{*\pm} \to D^0 + \pi^{\pm}_{slow} \to K^{\mp} + \pi^{\pm} + \pi^{\pm}_{slow}$. $D^{*\pm}$-meson production cross sections are measured in the kinematic range of $100\,\text{GeV}^2 < Q^2 < 1000\,\text{GeV}^2$, $0.02 < y < 0.7$, $-1.5 < \eta(D^*) < 1.5$ and $p_t(D^*) > 1.5\,\text{GeV}$.

The measured data are compared to results from next-to-leading order (NLO) calculations in the following schemes: The zero-mass variable-flavour-number scheme (ZMVFNS) [3] for energy scales much larger than the charm quark mass m_c. Near the heavy quark production threshold the fixed-flavour-number scheme (FFNS) [4] is applicable. A combination of both schemes for the full phase space is given by the generalised mass variable flavour number scheme (GMVFNS) [5]. In all calculations the parton evolution is performed according to the DGLAP equations. For the massive NLO calculations the FFNS PDF set MRST2004FF3 [6] is used and the CTEQ6.6M [7] parton densities are taken for the ZMVFNS calculations. The data are also compared to predictions of the LO Monte Carlo (MC) programs RAPGAP [8] and CASCADE [9]. Both simulations are based on leading order matrix elements with the higher order corrections implemented via parton showers. For RAPGAP parton evolution is calculated according to the DGLAP equations with the PDF set CTEQ65M and CASCADE implements the CCFM equations (k_t factorisation) with the unintegrated PDF set A0. The MCs are also used to estimate the detector response using a full simulation of the H1 detector. Details concerning the parameters of the calculations like the renormalisation scale and its variations for calculating the theoretical uncertainties are given in [2].

2. Cross section Measurement and Results

DIS events are selected by requiring the scattered electron in the main calorimeters of the H1 experiment. Its measurement and that of the hadronic final state is used to reconstruct the kinematics of the events (photon virtuality Q^2, Bjorken scaling variable x,...). Events with charm quarks are identified via full reconstruction of the "golden" decay channel $D^{*\pm} \to D^0 + \pi^{\pm}_{slow} \to K^{\mp} + \pi^{\pm} + \pi^{\pm}_{slow}$by measuring the tracks of the decay particles in the central track detector. The number of produced D* mesons is extracted by signal fits to invariant mass distributions [2, 10]. For the cross section determination the limited acceptances and efficiencies of the detector (in total $\sim 30\%$) are taken into account by correction factors calculated using RAPGAP and CASCADE

Monte Carlo samples. Initial and final QED radiation are taken into account adequately to get the visible cross sections at the Born level.

A total cross section in the visible range defined in Sec. 1 of

$$\sigma_{vis}^{tot}(e^{\pm}p \to e^{\pm}D^{*\pm}X) = 225 \pm 14\,(\text{stat.}) \pm 27\,(\text{syst.})\ \text{pb},$$

is observed. The corresponding prediction from HVQDIS amounts to 241 ± 15 which is in good agreement with the data. Fig. 1 shows the differential cross section as a function of Q^2 together

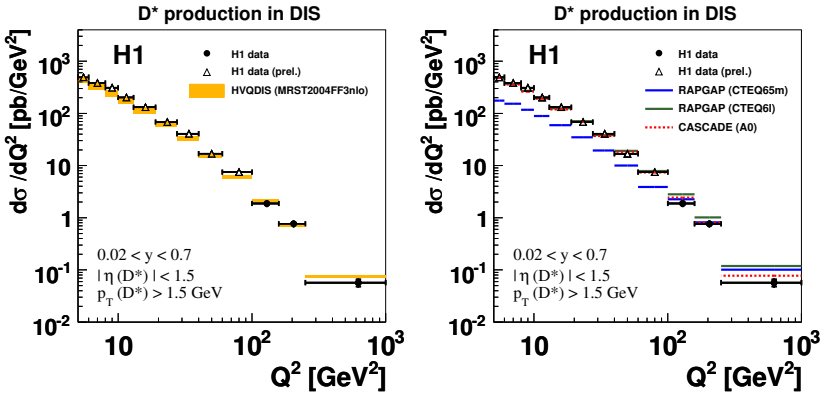

Figure 1: Measured differential cross section as a function of Q^2 together with the results from a medium Q^2 analysis [11].

with the preliminary result from the lower Q^2 analysis [11] in comparison with the NLO calculation (HVQDIS, left) and predictions from the LO MCs RAPGAP and CASCADE (right). The NLO calculation describes the Q^2 slope reasonably well over the full range. RAPGAP with the parton density CTEQ6LL [12] describes the data at medium Q^2 well, while the PDF set CTEQ6.5M gives a better description of the high Q^2 data. Neither of the PDF sets accounts for the slope over the full range in Q^2. In case of CASCADE which uses the PDF set A0 the description is much better. Fig. 2 shows the differential cross section as a function of $p_t(D^*)$ and $\eta(D^*)$ in comparison with HVQDIS, RAPGAP and CASCADE. The NLO calculation describes both distributions well

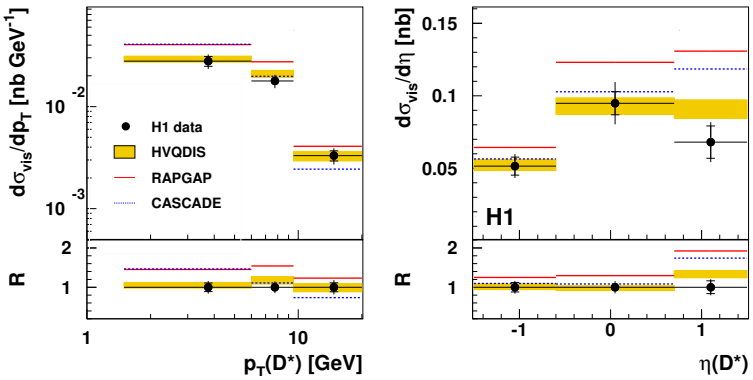

Figure 2: Differential cross sections as a function of $p_t(D^*)$ and $\eta(D^*)$, compared to LO and NLO pQCD predictions.

in contrast to the LO MCs RAPGAP and CASCADE. Especially CASCADE predicts a too soft $p_t(D^*)$ spectrum and both MCs overestimates the D^* production cross section at positive $\eta(D^*)$. The data are also compared to the ZMVFNS prediction [3]. This calculation is limited to a transverse $D^{*\pm}$ momentum in the photon-proton center-of-mass frame, $p_T^*(D^*)$, of $p_T^*(D^*) > 2\,\text{GeV}$. Therefore the same additional cut is applied to the data. In Fig. 3 the $D^{*\pm}$cross sections are shown as a function of Q^2 and $p_T(D^*)$ together with ZMVFNS and HVQDIS calculations. The ZMVFNS prediction fails to describe the data, while HVQDIS agrees well with the data.

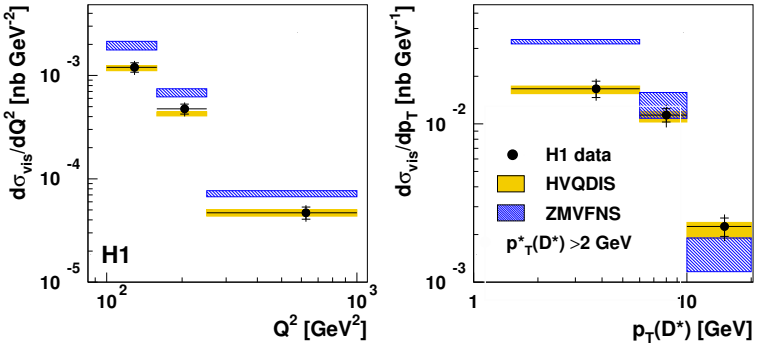

Figure 3: Differential cross sections as a function of Q^2 and $p_t(D^*)$ for $p_T^*(D^*) > 2\,\text{GeV}$, compared to NLO pQCD predictions.

The double differential cross sections in Q^2 and x are used to extract $F_2^{c\bar{c}}$ [10]. The extrapolation to the full phase space in $p_t(D^*)$ and $\eta(D^*)$ is done using HVQDIS with the parameters given in Sec. 1. The extrapolation factors $(\sigma_{tot}/\sigma_{vis})$ vary from 1.4 to 2.3 from bin to bin. The resulting $F_2^{c\bar{c}}$ is shown in Fig. 4 as a function of x for different values of Q^2. The $F_2^{c\bar{c}}$ values are consistent with those obtained using the H1 vertex detector information [13] whereas the expectation from the recent PDF fit to the inclusive DIS data, H1 PDF2009 [14] tend to overestimate the

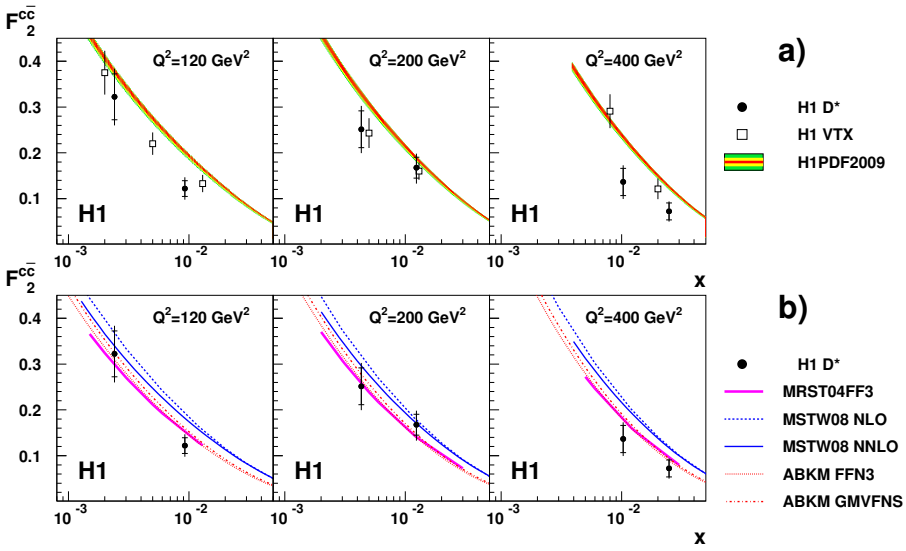

Figure 4: Extracted $F_2^{c\bar{c}}$ compared to NLO pQCD predictions

data. In Fig. 4 b) the measurements are compared to the massive FFNS calculation at NLO [4] (MRST04FF3) and NNLO [15] (ABKM) and to the GMVFNS predictions at NLO (MSTW08) and NNLO (MSTW08,ABKM) [15, 16]. The FFNS predictions agree well with the data over the full kinematic region investigated. The expectations for $F_2^{c\bar{c}}$ from a global fit in the GMVFNS at NLO tend to overestimate the data. At NNLO the GMVFNS prediction agrees better with the data.

3. Conclusion

Cross sections of $D^{*\pm}$ meson production have been measured for $Q^2 > 100\,\mathrm{GeV}^2$ and are compared to the predictions of Monte Carlo simulations and NLO calculations in massive and massless schemes. The NLO FFNS calculation HVQDIS agrees with the data well, while the calculation based on ZMVFNS fails to describe the data. Also the LO MCs shows deficiencies in some regions of the phase space. Further $F_2^{c\bar{c}}(x, Q^2)$ has been extracted by extrapolation of the measured cross sections to the full phase space using the massive NLO calculation (HVQDIS). The results are consistent with other measurements of $F_2^{c\bar{c}}$. The comparison of the data with NLO QCD predictions in different schemes indicates that the NLO FFNS provides the best description of charm production in the kinematic region investigated here.

References

[1] C. Adloff *et al.* [H1 Collaboration], Z. Phys. **C72** 593 (1996); C. Adloff *et al.* [H1 Collaboration], Nucl. Phys. **B545** 21 (1999); A. Aktas *et al.* [H1 Collaboration], Eur. Phys. J. **C51** 271 (2007).

[2] F. D. Aaron *et al.* [H1 Collaboration], Phys. Lett. B **686** (2010) 91 [arXiv:0911.3989 [hep-ex]].

[3] G. Heinrich, B. A. Kniehl, Phys. Rev. **D70** (2004) 094035 [hep-ph/0409303]; C. Sandoval, Ph.D. Thesis, University Hamburg (2009).

[4] B. W. Harris and J. Smith, Phys. Rev. **D57** (1998) 2806;

[5] R. S. Thorne and W. K. Tung, Proc. of the Workshop HERA and the LHC, DESY-PROC-2009-02 (2009) 332 ISBN 978-3-935702032-4 arXiv:0809.0714.

[6] A. D. Martin, W. J. Stirling and R. S. Thorne, Phys. Lett. **B636** (2006) 259 [hep-ph/0603143].

[7] P. M. Nadolsky *et al.*, Phys. Rev. **D78** (2008) 013004 [arXiv:802.0007].

[8] H. Jung, Comput. Phys. Commun. **86** 147 (1995)

[9] H. Jung and G. Salam, Euro. Phys. J. **C 19** 351 (2001).

[10] M. Brinkmann, Ph. D. Thesis, University of Hamburg (2010).

[11] H1Collaboration, H1prelim-08-072, https://www-h1.desy.de/publications/

[12] J. Pumplin *et al.*, JHEP **07** 012 (2002).

[13] F. D. Aaron *et al.* [H1 Collaboration], DESY-09-096, arXiv:0907.2643;

[14] F. D. Aaron *et al.* [H1 Collaboration], DESY-09-005, arXiv:0904.3513.

[15] S. Alekhin, J. Blümlein, S. Klein, S. Moch, arXiv:0908.3128

[16] R. S. Thorne, Phys. Rev. **D73** (2006) 054019 [hep-ph/0601245]; A. D. Martin, W. J. Stirling, R. S. Thorne, G. Watt, arXiv:0901.0002.